Supporting Information

A new-type high-entropy electrocatalyst with a pyrochlore structure for acid-water oxidation

Jinhui Zhang, Lei Shi*, Xianbing Miao, Liping Yang, and Shiming Zhou

Hefei National Research Center for Physical Sciences at the Microscale, University of Science and Technology of China, Hefei 230026, Anhui, P. R. China.

*E-mail: shil@ustc.edu.cn;

Phone: +86-551-63607924.

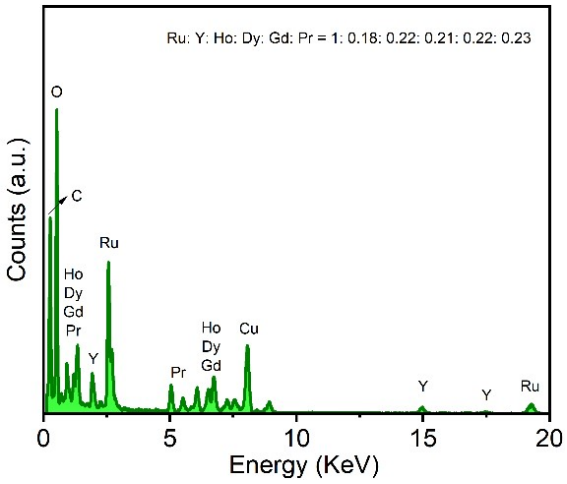

Figure S1. EDS spectrum of HE-YRO. The signals of Cu and C in the spectrum were originated from the copper grid coated by carbon membrane.

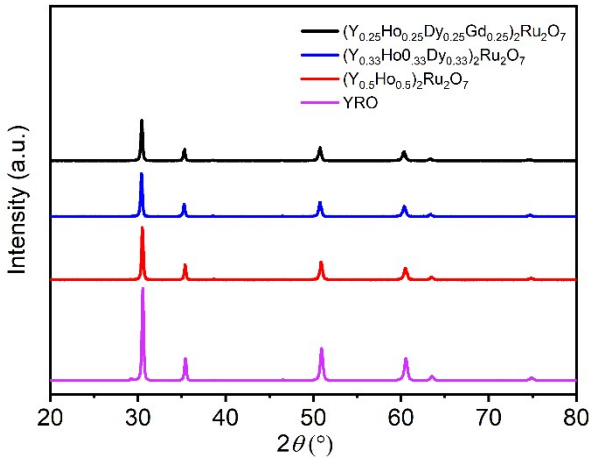

Figure S2. XRD patterns of YRO, $(Y_{0.5}Ho_{0.5})_2Ru_2O_7$, $(Y_{0.33}Ho_{0.33}Dy_{0.33})_2Ru_2O_7$, and $(Y_{0.25}Ho_{0.25}Dy_{0.25}Gd_{0.25})_2Ru_2O_7$.

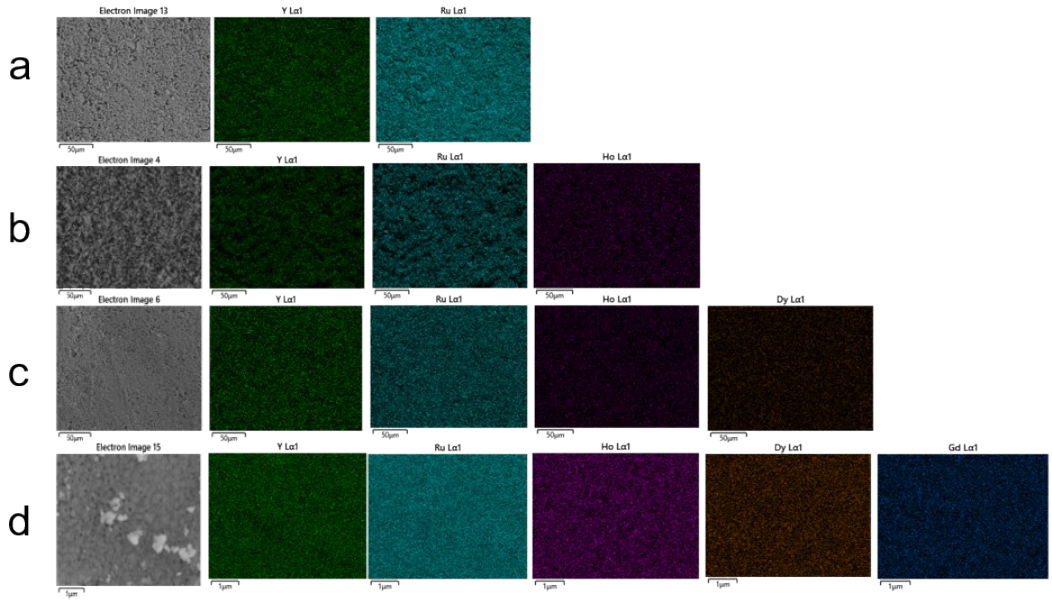

Figure S3. SEM-EDS mappings of (a) YRO, (b) $(Y_{0.5}Ho_{0.5})_2Ru_2O_7$, (c) $(Y_{0.33}Ho_{0.33}Dy_{0.33})_2Ru_2O_7$, and (d) $(Y_{0.25}Ho_{0.25}Dy_{0.25}Gd_{0.25})_2Ru_2O_7$.

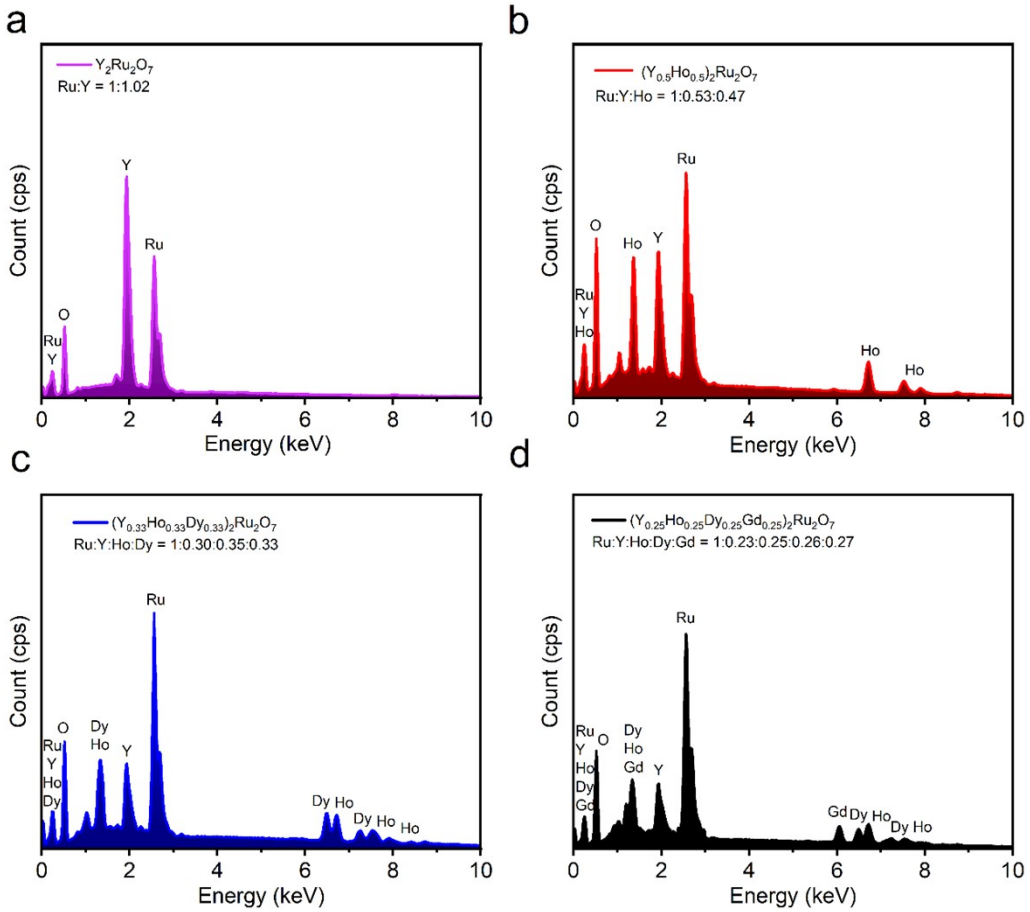

Figure S4. SEM-EDS spectra of (a) YRO, (b) $(Y_{0.5}Ho_{0.5})_2Ru_2O_7$, (c) $(Y_{0.33}Ho_{0.33}Dy_{0.33})_2Ru_2O_7$, and (d) $(Y_{0.25}Ho_{0.25}Dy_{0.25}Gd_{0.25})_2Ru_2O_7$.

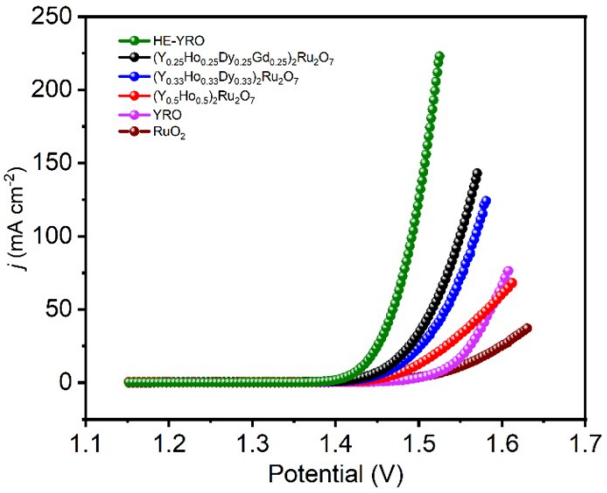

Figure S5. Polarization curves of as-prepared Ru-based catalysts and commercial RuO_2.

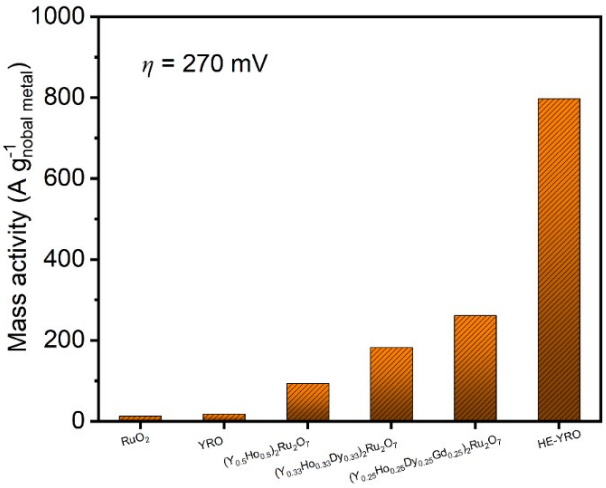

Figure S6. Comparison of mass activity at η = 270 mV.

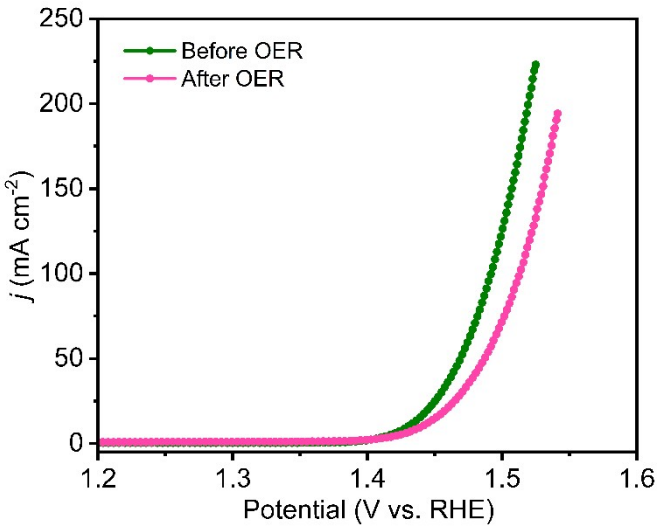

Figure S7. Polarization curves for HE-YRO before and after OER test.

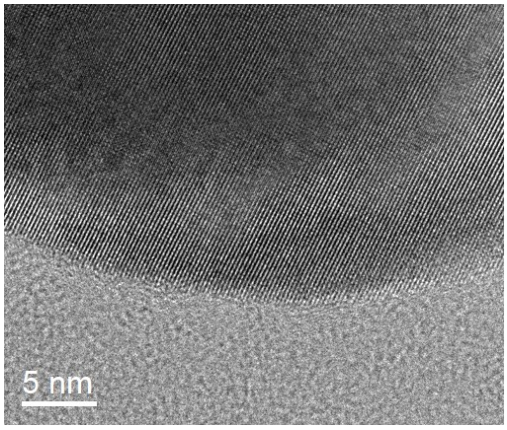

Figure S8. HRTEM image of the HE-YRO electrocatalyst after the stability test.

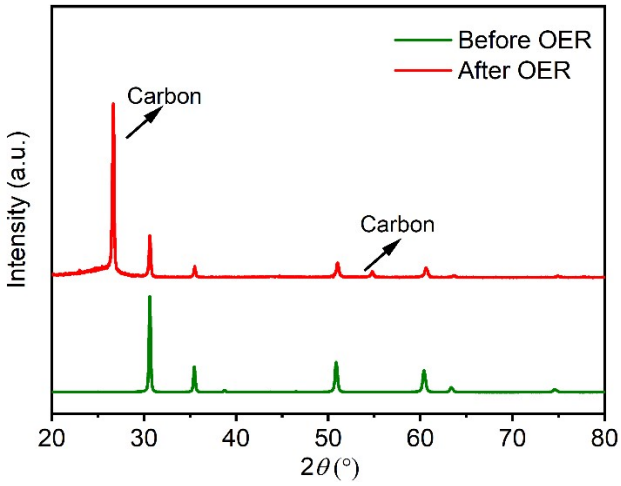

142

143 Figure S9. XRD patterns of HE-YRO before and after the OER testing.

144

145

146

147

148

149

150

151

152

153

154

155

156

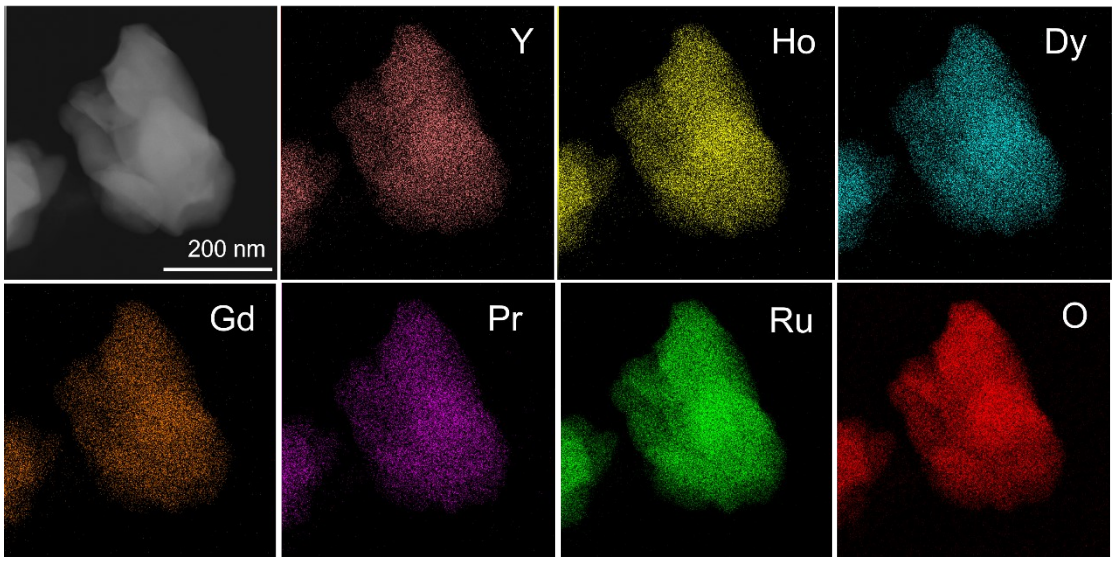

Figure S10. HRTEM-EDS elemental mappings of the HE-YRO sample after OER.

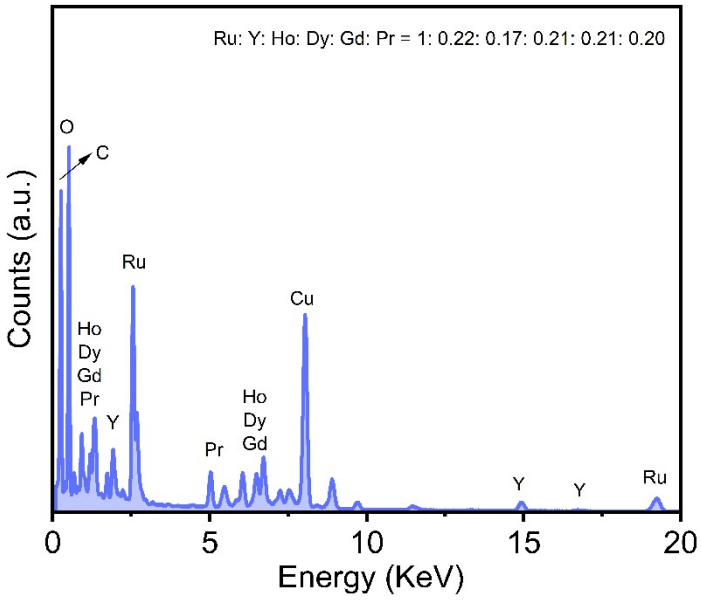

171

172 Figure S11. EDS spectrum of HE-YRO after OER. The signals of Cu and C in the

173 spectrum were originated from the copper grid coated by carbon membrane.

174

175

176

177

178

179

180

181

182

183

184

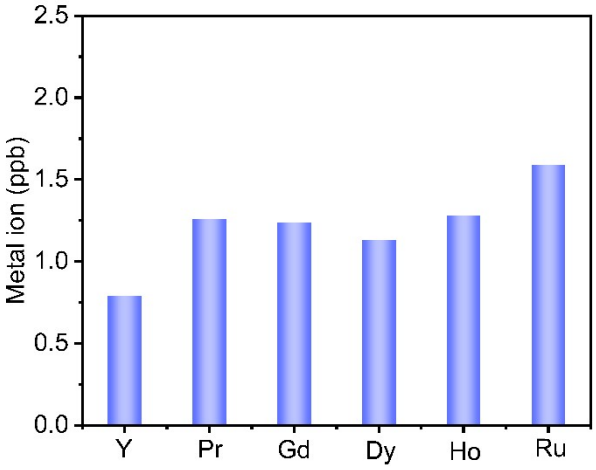

Figure S12. ICP analysis for HE-YRO after OER test.

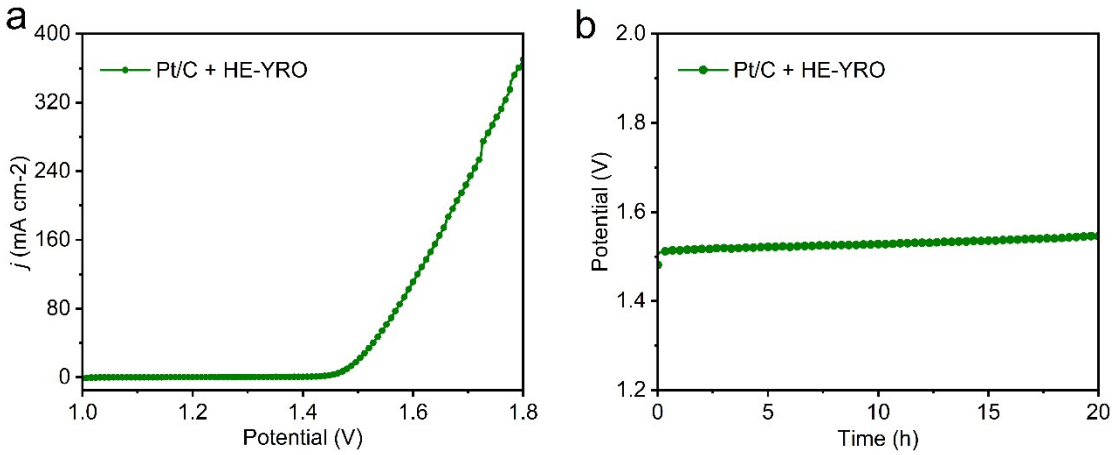

Figure S13. (a) Polarization curve of HE-YRO || Pt/C for overall water splitting. (b) Chronopotentiometric curve water electrolysis for the HE-YRO || Pt/C in a two-electrode setup with a current density of 10 mA cm^{-2}.

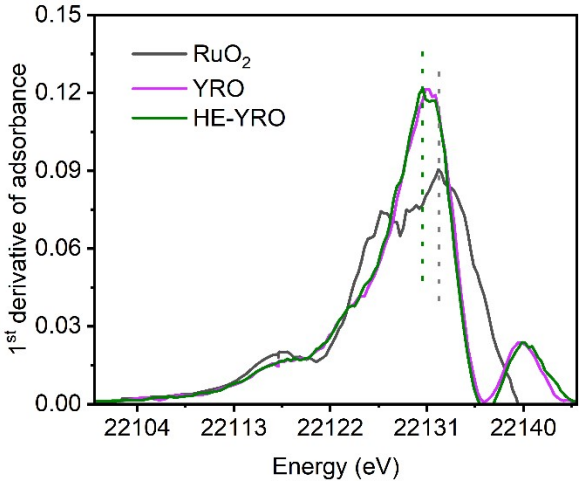

Figure S14. 1st derivative curves of Ru *K*-edge XANES spectra for HE-YRO, YRO, and RuO_2.

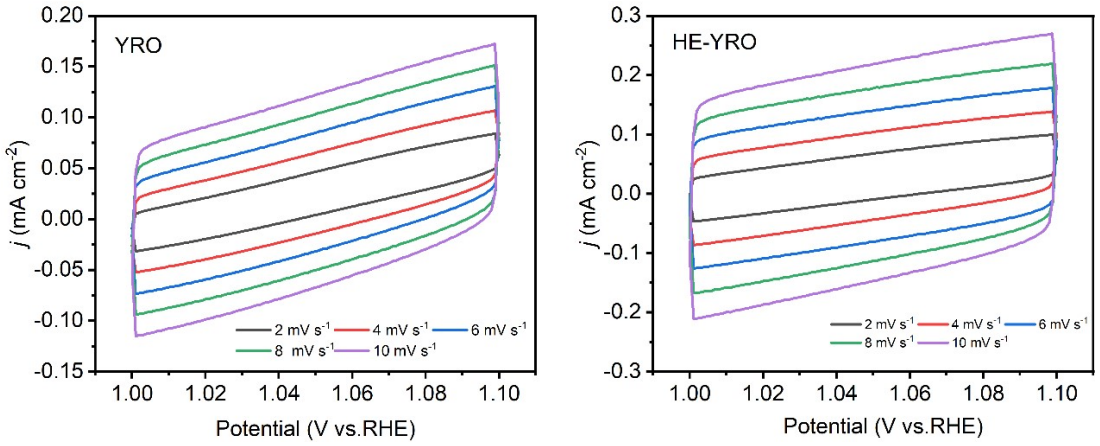

Figure S15. Cyclic voltammetry curves in O^2-saturated 0.5M H_2SO_4. The sweep rates are in the range of 2-10 mV s^{-1}.

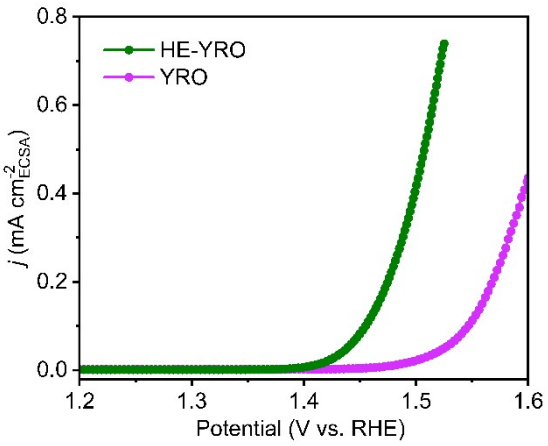

Figure S16. Polarization curves for HE-YRO and YRO normalized by ECSA.

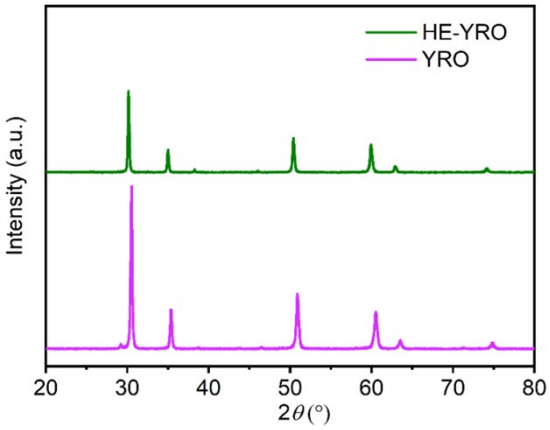

Figure S17. XRD patterns of HE-YRO and YRO.

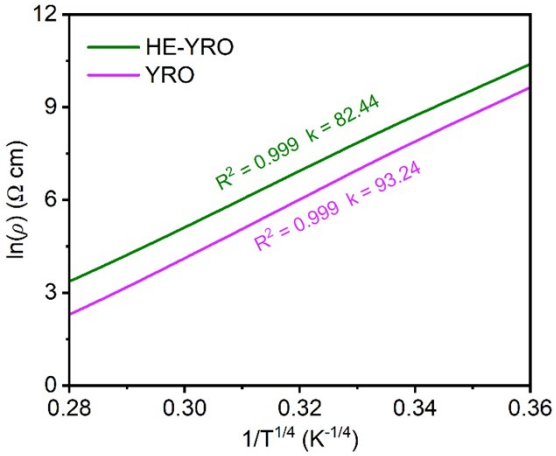

290

291 Figure S18. The ρ(T) curves fitted with the three-dimensional VRH model. The hopping energy W

292 ($W=0.25k_BT_0^{1/4}T^{3/4}$, where k_B is the Boltzmann constant) is proportional to $T_0^{1/4}$ ($k = T_0^{1/4}$).

293

294

295

296

297

298

299

300

301

302

303

304

305

306

307

308

309

310

311

312

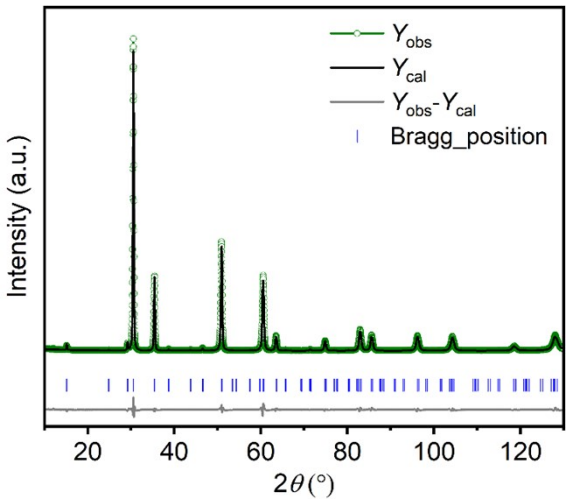

Figure S19. XRD pattern for YRO together with the Rietveld refined results.

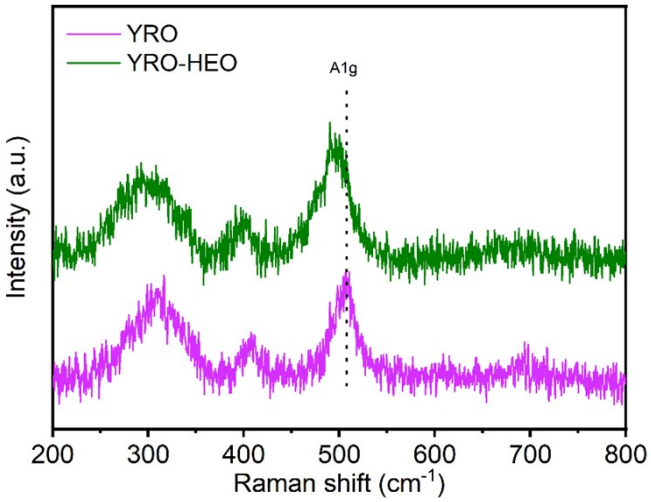

Figure S20. Raman spectra of HE-YRO and YRO.

Table S1. Refined structural parameters of the room temperature XRD patterns for HE-YRO and YRO samples.

Sample	HE-YRO	YRO
Space group	*Fd-3m*	
a (Å)	10.2121(4)	10.1449(1)
Cell volume (Å ^{3})	1064.9891(4)	1044.1030(2)
Ru-O bond (Å)	1.9856(6)	1.9964(8)
Ru-O-Ru bond angel (°)	130.78	127.86
R_p	5.93	6.41
R_{wp}	8.21	9.04

393 Table S2. Element ratios of the HE-YRO before OER test determined using ICP-AES.

Sample	Ru (at. %)	Y (at. %)	Ho (at. %)	Dy (at. %)	Gd (at. %)	Pr (at. %)
HE-YRO	50.3	9.7	10.1	9.6	9.9	10.4

394 The calculated molar ratio of Ru/Y/Ho/Dy/Gd/Pr is 1.00: 0.19: 0.20: 0.19: 0.20: 0.21

395

396

397

398

399

400

401

402

403

404

405

406

407

408

409

410 Table S3. Comparison of OER activities for the Ru-based catalysts in acid media.

Catalysts	η_{10} (mV)	Mass activity@ η (A g^{-1}@ mV)	Electrolytes	References
HE-YRO	200	797.1@270	0.5M H_2SO_4	**This work**
YRO	304	18.3@270	0.5M H_2SO_4	**This work**
$Y_{1.75}Ca_{0.25}Ru_2O_{7-\delta}$	275	597.85@270	0.5M H_2SO_4	S1
$Y_{1.85}Ba_{0.15}Ru_2O_{7-\delta}$	278	681.6@270	0.5M H_2SO_4	S2
MoO_x@$Y_2Ru_2O_{7-\delta}$	240	~300@270	0.1M $HClO_4$	S3
Y_2RuMnO_7	260	~100@270	0.1M $HClO_4$	S4
$Y_{1.7}Sr_{0.3}Ru_2O_7$	264	418@270	0.5M H_2SO_4	S5
S_H-RuCoO NRs	231	783@270	0.5M H_2SO_4	S6
RuIr-HEO	220	666.5@270	0.5M H_2SO_4	S7
$Ru_5W_1O_x$	235	750@300	0.5M H_2SO_4	S8
$RuNi_2$@G-250	227	120@300	0.5M H_2SO_4	S9
$Y_{1.75}Co_{0.25}Ru_2O_{7-\delta}$	275	~110@270	0.5M H_2SO_4	S10
$Ho_2Ru_2O_7$	280	~590@320	0.1M $HClO_4$	S11
Ru@IrO_x	282	644.8@330	0.5M H_2SO_4	S12
$Y_2[Ru_{1.6}Y_{0.4}]$ $O_{7-\delta}$	~240	~480@250	0.5M H_2SO_4	S13
$Y_{1.85}Zn_{0.15}Ru_2O_{7-\delta}$	291	412.7@320	0.5M H_2SO_4	S14
Au-Ru nanoparticles	220	-	0.5M H_2SO_4	S15
$RuTe_2$ nanorods	245	-	0.5M H_2SO_4	S16
RuRh@$(RuRh)O_2$	245	119.8@250	0.1M $HClO_4$	S17

411 (η_{10}: The overpotential of catalysts at 10 mA cm^{-2})

412

413

414

415

416

417

418

419

Table S4. XPS analysis of Ru $3p_{3/2}$ region of HE-YRO and YRO.

Species	HE-YRO		YRO	
	Peak position (eV)	Area (%)	Peak position (eV)	Area (%)
Ru^{4+}	463.25	76.6	463.25	85.9
Ru^{3+}	465.22	23.4	465.22	14.1
Ru^{3+}/Ru^{4+}	0.31		0.16	

Table S5. XPS analysis of O 1s region of HE-YRO and YRO.

Species	HE-YRO		YRO	
	Peak position (eV)	Area (%)	Peak position (eV)	Area (%)
O_L	529.1	27.55	529.1	28.00
O_{OH}	531.4	67.24	531.4	59.95
O_W	533.2	5.21	533.2	12.05
O_{OH}/O_L	2.44		2.14	

Reference

(S1). Q. Feng, Z. Zhao, X.-Z. Yuan, H. Li and H. Wang, *Appl. Catal. B: Environ.*, 2020, **260**, 118176.

(S2). Q. Feng, J. Zou, Y. Wang, Z. Zhao, M. C. Williams, H. Li and H. Wang, *ACS Appl. Mater. Interfaces*, 2020, **12**, 4520-4530.

(S3). T. Liu, H. Guo, Y. Chen, Z. Zhang and F. Wang, *Small*, 2023, **19**, 2206698.

(S4). D. Galyamin, J. Torrero, I. Rodríguez, M. J. Kolb, P. Ferrer, L. Pascual, M. A. Salam, D. Gianolio, V. Celorrio, M. Mokhtar, D. Garcia Sanchez, A. S. Gago, K. A. Friedrich, M. A. Peña, J. A. Alonso, F. Calle-Vallejo, M. Retuerto and S. Rojas, *Nat. Commun.*, 2023, **14**, 2010.

(S5). N. Zhang, C. Wang, J. Chen, C. Hu, J. Ma, X. Deng, B. Qiu, L. Cai, Y. Xiong and Y. Chai, *ACS Nano*, 2021, **15**, 8537-8548.

(S6). Q. Yao, Z. Yu, Y.-H. Chu, Y.-H. Lai, T.-S. Chan, Y. Xu, Q. Shao and X. Huang, *Nano Res.*, 2022, **15**, 3964-3970.

(S7). X. Miao, Z. Peng, L. Shi and S. Zhou, *ACS Catal.*, 2023, **13**, 3983-3989.

(S8). Y. Wen, C. Liu, R. Huang, H. Zhang, X. Li, F. P. Garcia de Arquer, Z. Liu, Y. Li and B. Zhang, *Nat. Commun.*, 2022, **13**, 4871.

(S9). X. Cui, P. Ren, C. Ma, J. Zhao, R. Chen, S. Chen, N. P. Rajan, H. Li, L. Yu, Z. Tian and D. Deng, *Adv. Mater.*, 2020, **32**, e1908126.

(S10). N. Han, S. Feng, Y. Liang, J. Wang, W. Zhang, X. Guo, Q. Ma, Q. Liu, W. Guo, Z. Zhou, S. Xie, K. Wan, Y. Jiang, A. Vlad, Y. Guo, E. M. Gaigneaux, C. Zhang, J. Fransaer and X. Zhang, *Adv. Func. Mater.*, 2023, **33**, 2208399.

(S11). J. Yan, J. Zhu, D. Chen, S. Liu, X. Zhang, S. Yu, Z. Zeng, L. Jiang and F. Du, *J. Mater. Chem. A*, 2022, **10**, 9419-9426.

(S12). J. Shan, C. Guo, Y. Zhu, S. Chen, L. Song, M. Jaroniec, Y. Zheng and S.-Z. Qiao, *Chem*, 2019, **5**, 445-459.

(S13). J. Kim, P. C. Shih, Y. Qin, Z. Al-Bardan, C. J. Sun and H. Yang, *Angew. Chem. Int. Ed.*, 2018, **57**, 13877-13881.

(S14). Q. Feng, Q. Wang, Z. Zhang, Y. Xiong, H. Li, Y. Yao, X.-Z. Yuan, M. C. Williams, M. Gu, H. Chen, H. Li and H. Wang, *Applied Catalysis B: Environmental*, 2019, **244**, 494-501.

(S15). L. Gloag, T. M. Benedetti, S. Cheong, Y. Li, X. H. Chan, L. M. Lacroix, S. L. Y. Chang, R. Arenal, I. Florea, H. Barron, A. S. Barnard, A. M. Henning, C. Zhao, W. Schuhmann, J. J. Gooding and R. D. Tilley, *Angew. Chem. Int. Ed.*, 2018, **57**, 10241-10245.

(S16). J. Wang, L. Han, B. Huang, Q. Shao, H. L. Xin and X. Huang, *Nat. Commun.*, 2019, **10**, 5692.

(S17). K. Wang, B. Huang, W. Zhang, F. Lv, Y. Xing, W. Zhang, J. Zhou, W. Yang, F. Lin, P. Zhou, M. Li, P. Gao and S. Guo, *J. Mater. Chem. A*, 2020, **8**, 15746-15751.